Developmental Neuroscience

Dev Neurosci
DOI: 10.1159/000348432

Received: August 16, 2012
Accepted after revision: January 23, 2013
Published online: April 4, 2013

Temporal Expression of Cytokines and Signal Transducer and Activator of Transcription Factor 3 Activation after Neonatal Hypoxia/Ischemia in Mice

K. Shrivastava[a, c] G. Llovera[a, c] M. Recasens[a, c] M. Chertoff[a, c]
L. Giménez-Llort[b, c] B. Gonzalez[a, c] L. Acarin[a, c]

Departments of [a]Cell Biology, Physiology and Immunology and [b]Psychiatry and Forensic Medicine, and [c]Institute of Neuroscience, Universitat Autonoma Barcelona, Bellaterra, Spain

Key Words

Phosphorylated signal transducer and activator of transcription factor 3 · Interleukin-6 · Interleukin-1β · Interleukin-4 · Interleukin-13 · Interleukin-10 · Hypoxia/ischemia · Neonatal brain

Abstract

Hypoxia/ischemia (HI) is a prevalent reason for neonatal brain injury with inflammation being an inevitable phenomenon following such injury; but there is a scarcity of data regarding the signaling pathway involved and the effector molecules. The signal transducer and activator of transcription factor 3 (STAT3) is known to modulate injury following imbalance between pro- and anti-inflammatory cytokines in peripheral and central nervous system injury making it a potential molecule for study. The current study investigates the temporal expression of interleukin (IL)-6, IL-1β, tumor necrosis factor-α, IL-1ra, IL-4, IL-10, IL-13 and phosphorylated STAT3 (pSTAT3) after carotid occlusion and hypoxia (8% O_2, 55 min) in postnatal day 7 C57BL/6 mice from 3 h to 21 days after hypoxia. Protein array illustrated notable changes in cytokines expressed in both hemispheres in a time-dependent manner. The major pro-inflammatory cytokines showing immediate changes between ipsi- and contralateral hemispheres were IL-6 and IL-1β. The anti-inflammatory cytokines IL-4 and IL-13 demonstrated a delayed augmentation with no prominent differences between hemispheres, while IL-1ra showed two distinct peaks of expression spread over time. We also illustrate for the first time the spatiotemporal activation of pSTAT3 (Y705 phosphorylation) after a neonatal HI in mice brain. The main regions expressing pSTAT3 were the hippocampus and the corpus callosum. pSTAT3+ cells were mostly a subpopulation of activated astrocytes (GFAP+) and microglia/macrophages (F4/80+) seen only in the ipsilateral hemisphere at most time points studied (till 7 days after hypoxia). The highest expression of pSTAT3+ cells was observed to be around 24–48 h, where the presence of pSTAT3+ astrocytes and pSTAT3+ microglia/macrophages was seen by confocal micrographs. In conclusion, our study highlights a synchronized expression of some pro- and anti-inflammatory cytokines, especially in the long term not previously defined. It also points towards

K.S. and G.L. contributed equally to this work. The work is dedicated to Dr. Laia Acarin, a brilliant scientist, who deceased during the preparation of the manuscript.

KARGER

E-Mail karger@karger.com
www.karger.com/dne

0378–5866/13/0000–0000$38.00/0

Kalpana Shrivastava
Medical Histology, Torre M5
Department of Cell Biology Physiology and Immunology
Universitat Autonoma Barcelona, ES–08193 Bellaterra (Spain)
E-Mail Kalpana.Shrivastava@uab.cat

a significant role of STAT3 signaling following micro- and astrogliosis in the pathophysiology of neonatal HI-related brain injury. In the study, a shift from pro-inflammatory to anti-inflammatory cytokine profile was also noted as the injury progressed. We suggest that while designing efficient neuroprotective therapies using inflammatory molecules, the time of intervention and balance between the pro- and anti-inflammatory cytokines must be considered.

Introduction

Injury to the newborn during the perinatal stage is the underlying etiology for a host of developmental disabilities that includes spastic motor deficits such as cerebral palsy [1, 2] or other cognitive, behavioral, attentional, socialization and learning difficulties [3–6]. As brain development substantially influences the progression and signature outcomes of brain injury [7, 8], there is no guaranty of equivalent success in applying therapeutic procedures used for adult ischemia to the newborns. Nowadays, hypothermia is the main clinical therapy applied to infants that had suffered a perinatal brain injury but its efficiency depends on the severity of the damage [9]. In recent years, some studies have focused on the role of cytokines in the evolution of injury suggesting anti-inflammatory therapies to reduce neurodegeneration and tissue damage after an acute damage in the central nervous system [10, 11].

During the development of perinatal brain injury, tissue damage and neurodegeneration initiate a cascade of inflammatory responses depending on the nature and extent of damage. This is usually characterized by the involvement of damaged neurons, microglial cells, astrocytes, endothelial cells, recruited blood leukocytes and various cytokines [12–16]. Although the function of glial cells in the neonatal brain has been intensively studied during the last decade [17–19], the data on molecular mechanisms and the role of glial cells in a central nervous system injury in neonates are still inadequate.

Cytokines are involved in numerous functions, such as maintaining homeostasis, regulating immune cell proliferation and differentiation along with adjusting inflammatory cell function and the respective phenotype. Moreover, pro-inflammatory cytokines are implicated in the activation of the JAK/STAT pathway activating the STAT (signal transducer and activator of transcription) proteins [20, 21] that play a role in inflammatory response. Once STAT proteins are activated by phosphorylation, they dimerize to translocate into the nucleus [22, 23], where they bind to the DNA, triggering the expression of pro- and anti-inflammatory molecules that might aggravate or reduce the damage produced in the brain. Within the family of the STATs, STAT3 is described as an anti-inflammatory protein in adults although its activation mechanism in neonates remains unclear [24]. STAT3 is activated by some interleukins such as interleukin (IL)-6, IL-11, IL-10, IL-20 and IL-22 [25, 26]. Furthermore, its activation induces cellular stress, immune cell activation, inflammation, cell migration, astrocyte interaction, neurodevelopment, axonal growing, neurodegeneration, anti-apoptosis and neuroprotection [27–29].

In this regard, it becomes evident that the expression of cytokines, the pattern of distribution of phosphorylated STAT3 (pSTAT3) and its anti-inflammatory role after perinatal brain damage will provide us with new lines to counter perinatal brain injury. In the present study, we have used the experimental model of hypoxia/ischemia (HI)-induced neonatal injury first described by Vannucci and coworkers [30, 31] for the rat, and later adapted to the mouse by others [32–34]. Injury was induced in postnatal day (P) 7 mice and followed at different survival times, focusing both on the ipsilateral (IL) and the contralateral (CL) hemispheric changes. Our objective was to perform a quantitative analysis of different cytokines and characterize the expression pattern of pSTAT3 as a response to HI-induced neonatal injury. Importantly, the study of the temporal correlation between STAT3 phosphorylation and the cytokines produced aims to help in the future design and development of novel neuroprotective strategies.

Materials and Methods

Animals

C57BL/6 mice (bred in Harlan Labs, France) of different postnatal ages were used for all experiments. Animals were maintained at a constant temperature (24 ± 2°C) and housed on a 12-hour light:12-hour dark cycle with food and water ad libitum. Experimental animal work was conducted in accordance with the ethical commission of the Autonomous University of Barcelona, in compliance with Spanish regulations and the European Union directives on the use of animals in scientific research. All efforts were made to minimize the number and suffering of animals used at each stage of experimentation.

Hypoxic/Ischemic Injury Model

HI brain damage was induced in P7 mice by permanent left carotid occlusion and exposure to hypoxia as described and standardized elsewhere [19, 35]. Briefly, a midline ventral skin incision was made under isoflurane anesthesia (4.5% v/v for induction and

Table 1. List of antibodies and dilutions used in this study

Target antigen			Dilution	Applications	Catalogue number, brand
Primary antibodies	pSTAT3 (Tyr705)	rabbit monoclonal	1:250, 1:1,000	IF, WB	9145, (D3A7) XP, Cell Signaling
	GFAP	mouse monoclonal	1:1,000, 1:7,000	IF, WB	G3893, Sigma Aldrich
	F4/80	rat monoclonal	1:500	IF	MCA497G, AbD Serotec
	Actin	mouse monoclonal	1:4,000	WB	A5441, Sigma Aldrich
	Lamin B	goat polyclonal	1:3,000	WB	sc-6217 (M-20), Santa Cruz Biotechnologies
Secondary antibodies	Alexa 488	anti rat	1:500	IF	A11006, Invitrogen
	Alexa 568	anti rabbit	1:500	IF	A10042, Invitrogen
	Cy5	anti mouse	1:500	IF	PA45001, Amersham Biociences
	HRP	anti rabbit	1:4,000	WB	G21234, Invitrogen
	HRP	anti mouse	1:4,000	WB	NA931V, Amersham Biociences
	HRP	anti goat	1:4,000	WB	HAF019, R&D System
DAPI			1:10,000	IF	D9542, Sigma Aldrich
pSTAT3 (Y705) blocking peptide			25×	IF	1195, Cell Signaling

2.5% v/v for maintenance, and 0.6 l/min of O_2); the left carotid artery was exposed and sutured with an 8-0 silk surgical suture. After surgery, pups were returned to their dam for 1.5–2 h to recover. Later, litters were placed for 55 min in a hypoxic chamber containing 8% of oxygen balanced with nitrogen, with controlled humidity and temperature maintained at 37°C. Pups were then kept back with their dams until sacrifice.

Groups and Tissue Processing

Control intact mice were sacrificed at P7, P10, P14, P21 and P30. Lesioned pups were sacrificed at 3, 12, 24, 48 and 72 h and at 7, 14 and 21 days after hypoxia. The animals used in all groups were from at least 3 different litters. Animals were grouped for comparison and analysis with respective age-matched controls as follows: group I – P7 mice with mice 3, 12, 24 and 48 h after hypoxia; group II – P10 mice with mice 72 h after hypoxia; group III – P14 mice with mice 7 days after hypoxia; group IV – P21 mice with mice 14 days after hypoxia, and group V – P30 mice with mice 21 days after hypoxia.

For immunohistochemical analysis, mice were anesthetized intraperitoneally (ketamine and xylazine 80/10 mg/kg) and intracardially perfused using 4% paraformaldehyde in phosphate-buffered saline (pH 7.4). Subsequently, brains were removed, postfixed for 4 h in the same fixative, cryoprotected in 30% sucrose, frozen with dry CO_2, and finally stored at –80°C until use. Brains were serially cut in a cryostat (Leica CM3050 S) into 30-µm-thick sections and stored mounted on Flex IHC slides (K8020, Dako) at –20°C.

For Western blotting and protein array, another set of animals was intracardially perfused using cold phosphate-buffered saline. Brains were carefully dissected (cerebellum and olfactory bulb removed) separating the IL and CL hemisphere, quickly frozen in liquid nitrogen and stored at –80°C until use. Tissues were homogenized and the nuclear fraction was separated using the Nuclear Extraction Kit (40410, Active Motif). Whole-cell protein extract for protein array was prepared by homogenizing the tissue in the lysis buffer [50 mM Tris-HCl, pH 7.6, 150 mM NaCl, 5 mM $CaCl_2$, 0.05% BRIJ35, 0.02% NaN_3, 1% Triton X-100 and protease inhibitor cocktail (P8340, Sigma)]. Lysate was centrifuged for 10 min at 14,000 rpm and supernatants were stored at 80°C. Protein was estimated using the bovine serum albumin protein assay kit (23225, Thermo Scientific). Western blotting samples were prepared by boiling at 90°C for 5 min with NuPAGE-LDS (0007, Invitrogen) sample buffer. The animals used in all groups (n = 3–5) were from at least 3 different litters.

Protein Array

The cytokines IL-1β, tumor necrosis factor (TNF)-α, IL-6, IL-1ra, IL-4, IL-10 and IL-13 were analyzed using a SearchLight® Custom Mouse 7-Plex Array (85687, Aushon Biosystems) according to the manufacturer's instructions. Briefly, 50 µl whole-cell extracts were diluted with sample diluent (1:1) and were added in the custom plates along with standards in separate wells for overnight incubation at 4°C. The plates were then washed thrice with wash buffer (1×). Samples were further incubated with 50 µl of biotinylated antibody reagent for 2 h at room temperature (RT) in a rocking platform at 200 rpm. Subsequently, the plates were washed and 50 µl of streptavidin-horseradish peroxidase reagent was added to be incubated at RT in a rocking platform at 200 rpm for 30 min. Following 3 washes, 50 µl of SuperSignal® Substrate was added to detect the luminescent enzyme-substrate reaction. A cooled CCD camera (at 22°C) was used to read the plate 10 min after substrate addition. Images were analyzed using Aushon SearchLight Array Analyst software. All data were corrected as picograms/milligram of protein.

Immunohistochemistry

Slides for immunohistochemistry were selected according to the optimal injury score as defined in our previous study [19]. To characterize cells expressing pSTAT3, triple immunofluorescence was performed using astrocyte (glial intermediate filament protein, GFAP) and microglia/macrophage (F4/80) markers (table 1). Briefly, sections on slides were washed with Tris-buffered saline (TBS) containing 0.3% Triton X-100 (TBS-T, pH 7.4).

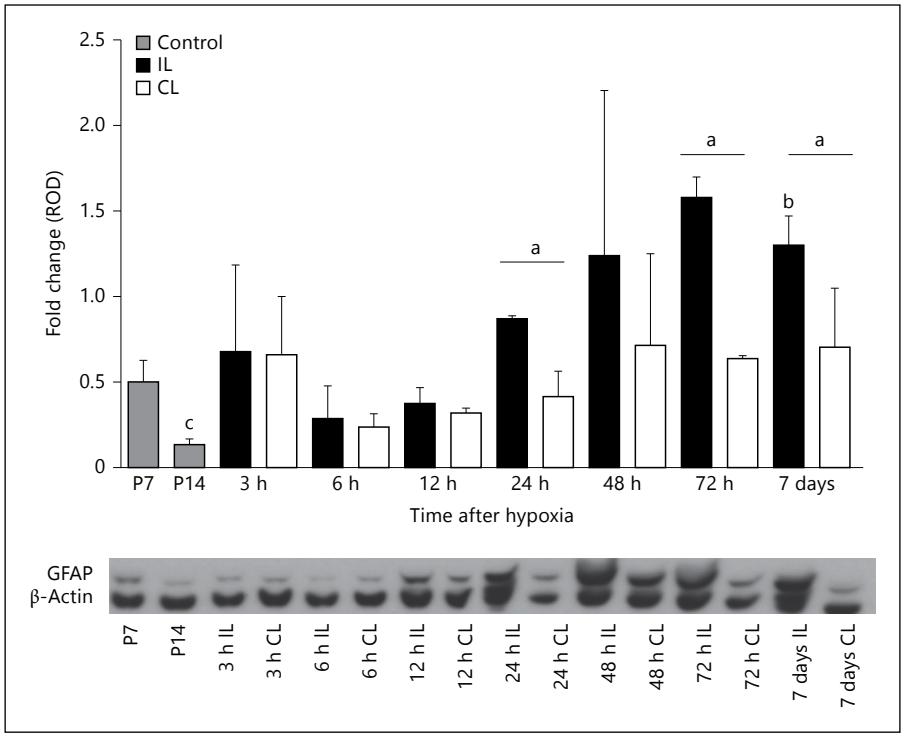

Fig. 1. Changes in GFAP expression after HI in the neonatal brain. Western blot was performed on brain samples following HI and were densitometrically compared to the age-matched controls (P7 and P14). Representative Western blot of GFAP and β-actin, the latter used for normalization of protein loading shown in the graph as relative optical density (ROD). Data are shown as means ± SEM. t test, [a] $p < 0.05$, for IL versus CL comparison and showing differences with respect to P7. ANOVA, followed by the Bonferroni post hoc test, was used ([b] $p < 0.05$; vs. respective controls). [c] $p < 0.05$: comparison between controls.

Sections were then incubated in blocking buffer (BB: 10% fetal calf serum, 0.3% bovine serum albumin in TBS-T) at RT for 1 h followed by incubation with the primary antibodies prepared in BB, namely, anti-pSTAT3, anti-GFAP and anti-F4/80 (table 1) overnight at 4°C and 1 h at RT. pSTAT3 blocking peptide was used on a separate slide to ensure the specificity of pSTAT3 antibody (no staining was observed in this condition). Samples were rinsed again in TBS-T and incubated for 1 h at RT with corresponding secondary antibodies (table 1). Further sections were rinsed and stained with DAPI (4′,6-diamidino-2-phenylindole) and finally after rinsing they were dehydrated and coverslipped with DPX. Samples were then analyzed with a confocal Leica-Sp5 or Leica-Sp2 microscope. Contrast and brightness adjustments for figures were made, and final plates were composed using Adobe Photoshop CS.

Western Blotting

pSTAT3 and GFAP levels were quantified by Western blotting using 30 μg protein from nuclear extract or whole-cell extract, respectively. Proteins were separated on 4–12% gradient ready-to-use NuGel (WG1403, Invitrogen) and transferred to nitrocellulose membrane (IB3010-01, Invitrogen). The membranes were blocked in BB [5% nonfat dry milk (sc-2325, Santa Cruz Biotechnology), in TBS + 0.1% Tween 20 (93773, Sigma)] for 1 h at RT followed by incubation with the respective primary antibody (table 1) in the same BB overnight at 4°C and 2 h at RT. The membranes were then washed with TBS-T and incubated with respective secondary antibodies conjugated to horseradish peroxidase (table 1) prepared in BB. Bound antibodies were then visualized by chemiluminescence substrate (34080, Thermo Scientific for GFAP and 170-5070, Bio-Rad for pSTAT3). The membranes were stripped using stripping buffer (21059, Thermo Scientific) and reprobed with Lamin B (nuclear extract) or β-actin (whole-cell extract) antibody to ensure equal loading in all wells. Lamin B was shown and analyzed according to Kolbus et al. [36]. The bands were analyzed using ImageJ (NIH) and the results were expressed as mean ± SEM of several membranes.

Statistical Analysis

Graphpad, Prism 3 software was utilized for all analysis. To study the differences between controls and IL/CL hemispheres after hypoxia unpaired Student's t test (with Welch's correction, if necessary) was used, while one-way ANOVA followed by Dunnett's post hoc analysis was used to study the effect of lesion. Data are presented as mean ± SEM. The data were considered significantly different at p value <0.05.

Results

GFAP Increased after HI Injury in Neonatal Mice

We first performed a Western blot analysis to quantify GFAP following damage produced by HI in the neonatal brain. An antibody to GFAP detected a single 50-kDa protein band in samples of control and injured brains (fig. 1). Densitometric analysis of GFAP bands revealed a decrease in the expression of GFAP at P14 with respect to

P7 (fig. 1; between controls). HI increased the expression of GFAP in the IL compared to the CL hemisphere and statistical significance was achieved at 24 h, 72 h and 7 days after hypoxia (fig. 1; IL vs. CL). Additionally, the overexpression of GFAP persisted in the IL side at 7 days after HI, showing statistical significance compared with P14 (fig. 1; control vs. time points after hypoxia).

Modulation of Pro-Inflammatory Cytokines in Neonatal Brain after HI

Expression of Pro-Inflammatory Cytokines in the Control Postnatal Brain

IL-1β protein expression was not detected during postnatal development (fig. 2A). In contrast, TNF-α expression was only observed at P14, showing significant differences with respect to P7 (fig. 2B; between controls). However, IL-6 is constituently expressed at low levels in the control postnatal brain (fig. 2C). No expression was observed at P21 and P30 (data not shown)

HI-Induced IL-1β Expression

Hypoxia induced the expression of IL-1β as early as 3 h after hypoxia in both hemispheres and at almost all the time points evaluated (fig. 2A; vs. respective controls). At 6 h after hypoxia, differences between the IL and CL hemisphere were observed (fig. 2A; IL vs. CL), demonstrating a cumulative effect of ischemia at this time point. Additionally, the effect of HI was significantly different in the IL hemisphere at 3 h compared to 6 h (fig. 2A; vs. 3 h after hypoxia) and also at 6 h versus 48 h and 7 days (fig. 2A; vs. 6 h after hypoxia). No expression was observed at 14 days after hypoxia or at longer time points studied (data not shown).

TNF-α Is Induced Mainly in the IL Hemisphere

TNF-α protein was detected as soon as 3 h after hypoxia, showing a significant increase in comparison to the age-matched control on the IL side that persisted till 72 h of damage. Although delayed with respect to the IL hemisphere, the CL hemisphere also showed significant changes of TNF from 12 h to 7 days (fig. 2B; vs. respective controls). There was no significant difference in this cytokine between the two hemispheres. The TNF-α expression was undetectable at 14 days after hypoxia or at longer time points (data not shown).

Early as Well as Delayed Changes in IL-6 Expression Were Observed after HI

IL-6 expression increased after hypoxia at almost all time points in both hemispheres compared to age-matched controls (fig. 2C; vs. respective controls). Interestingly, an earlier peak of expression for IL-6 was detected around 3–6 h after hypoxia on the IL side in comparison to the CL hemisphere (fig. 2C; IL vs. CL). After a slight downregulation, a second round of augmentation in IL-6 levels can be noted at 48 h in both hemispheres. The levels again declined at different rates, being slower on the IL side compared to the CL hemisphere. Levels were significantly different at 7 days after hypoxia (fig. 2C; vs. 12 h and vs. 24 h). These results demonstrated two waves in the effects of HI in the modulation of IL-6, one from 3 to 6 h and the other from 48 h that also affects the CL hemisphere. No IL-6 expression was observed at 14 days after hypoxia or at longer time points studied (data not shown).

Modulation of Anti-Inflammatory Cytokines

Expression of Anti-Inflammatory Cytokines in the Control Postnatal Brain

IL-1ra, IL-4 and IL-10 were detected at low levels from P7 to P14 in the control brain (fig. 2D, E, G, respectively). However, IL-13 was not detected in the control postnatal brain (fig. 2F). No expression was detected at P21 and P30 (data not shown).

IL-1ra Expression Is Highly Regulated by HI

HI mainly regulated the expression of IL1-ra, depicting two different temporal windows. An early increase was observed in the IL hemisphere from 3 to 6 h after hypoxia, being significantly different from the CL side in the later time point (fig. 2D; IL vs. CL). Interestingly, a delayed increase in the expression of IL-1ra in the IL hemisphere was evident from 48 h that persisted till 7 days after hypoxia (fig. 2D). A maximal expression was achieved in the IL hemisphere at 72 h being considerably higher compared to all the other time points (fig. 2; vs. 3–48 h after hypoxia). However, in the CL hemisphere, the IL-1ra expression remained comparable to controls (fig. 2D; vs. respective controls), except at 6 and 72 h after hypoxia (in accordance with IL peaks). The IL-1ra expression was undetectable from 14 days after hypoxia onwards (data not shown).

IL-4 Expression Was Affected by Hypoxia

Only hypoxia is sufficient to significantly increase the expression of IL-4 from 3 to 48 h after hypoxia in comparison to control (fig. 2E; vs. respective controls). However, in the IL hemisphere, the expression persists even at 72 h after hypoxia. From 7 days, there was no difference in the levels of IL-4 in both hemispheres with respect to control and

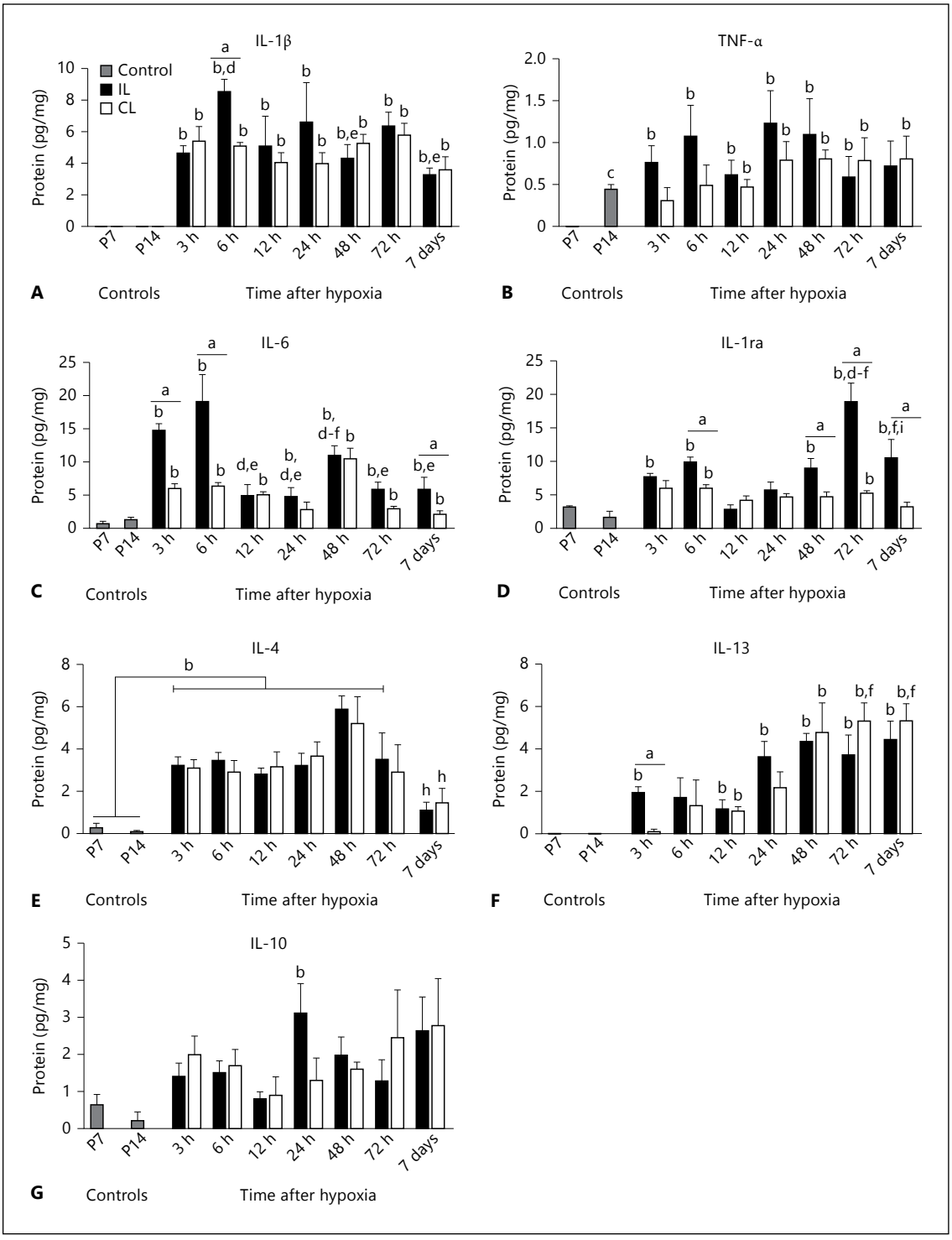

Fig. 2. Changes in cytokine levels in control animals (P7 and P14) and after neonatal HI from 3 h to 7 days after lesion. Quantification of pro-inflammatory cytokines, such as IL-1β (**A**), TNF-α (**B**), IL-6 (**C**), and anti-inflammatory cytokines including IL-1ra (**D**), IL-4 (**E**), IL-13 (**F**) and IL-10 (**G**) was made with respect to the age-matched controls. Data are means ± SEM. The significance among time points (ipsilateral) was represented as: d = versus 3 h; e = versus 6 h; f = versus 12 h; g = versus 24 h; h = versus 48 h, and i = versus 72 h after hypoxia. The data were considered significant at $p < 0.05$: [a] $p < 0.05$, IL versus CL; [b] $p < 0.05$, versus respective controls; [c] $p < 0.05$, comparison between controls.

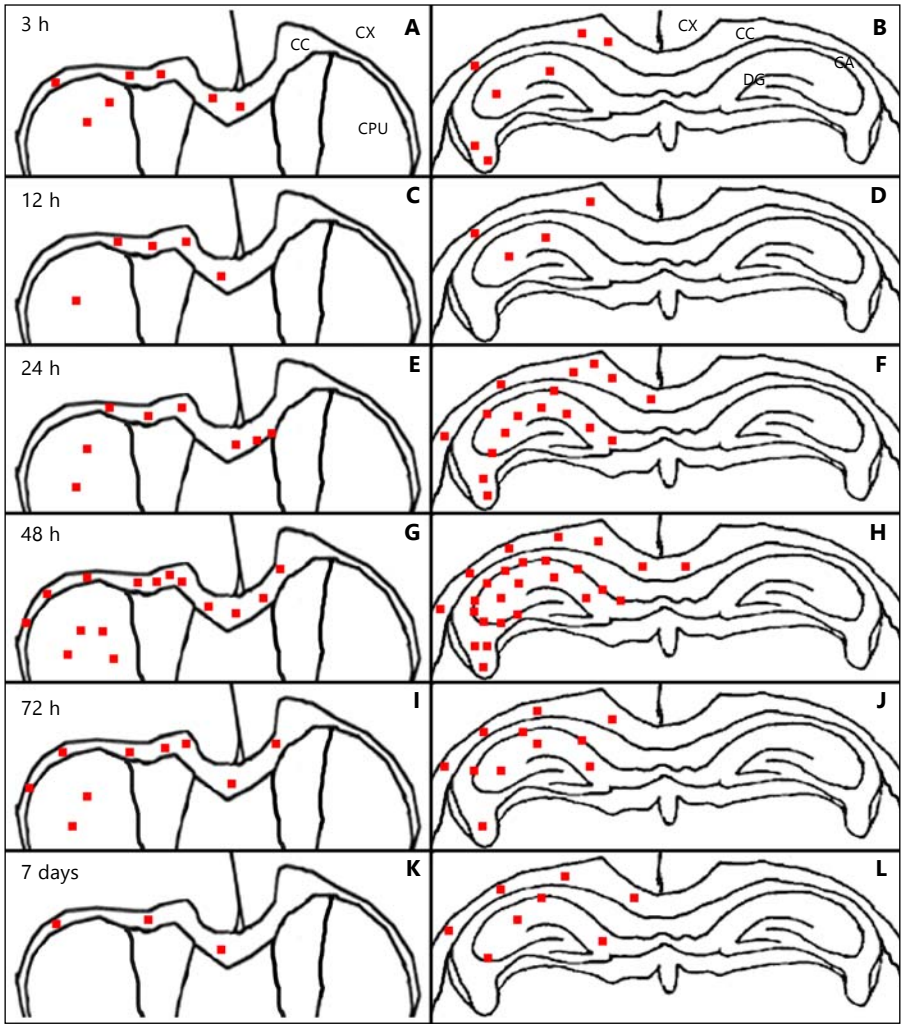

Color version available online

Fig. 3. Pattern of expression of pSTAT3 after HI. Diagram of anterior (left) and posterior (right) regions of the brain at 3 h (**A**, **B**), 12 h (**C**, **D**), 24 h (**E**, **F**), 48 h (**G**, **H**), 72 h (**I**, **J**) and 7 days (**K**, **L**) after HI. The red squares depict the distribution of pSTAT3+ cells. cx = Cortex; CPU = caudate and putamen; CA = cornu ammonis; DG = dentate gyrus. For colors, see online version.

earlier time points except with 48 h (fig. 2E; vs. respective controls, vs. 48 h after hypoxia). There was no additional effect of ischemia observed. No IL-4 expression was observed at longer time points studied (data not shown).

IL-13 Expression Was Induced after HI

As soon as 3 h after hypoxia, a notable IL-13 expression was induced in the IL hemisphere (fig. 2F; vs. control, IL vs. CL). From 12 h to 7 days, IL-13 increased slowly in both hemispheres, being the highest from 72 h to 7 days especially in the CL hemisphere when compared to 12 h after hypoxia (fig. 2F; vs. respective controls, vs. 12 h after hypoxia). Interestingly, only at 3 h after hypoxia did we observe differences between the IL versus CL hemispheres. No IL-13 expression was observed at longer time points (data not shown).

IL-10 Expression Slightly Changed after HI

HI injury produced an increase only in the IL hemisphere 24 h after hypoxia; however, this increase was not enough to be significantly different from the CL hemisphere (fig. 2G). No notable changes were observed at other time points. No expression was observed 14 days after hypoxia or longer time points (data not shown).

HI Differentially Expressed pSTAT3 in White and Gray Matter

The distribution of pSTAT3+ cells in the damaged brains has been summarized in figure 3, where they are depicted as red squares. No pSTAT3+ staining was detected in the control animals (fig. 4B–C, 5B, C). Confocal micrographs showing the distribution of pSTAT3+ cells in the corpus callosum (CC) and in the hippocampus are

shown in figures 4 and 5, respectively. The cells appeared to have maximum expression of STAT3 phosphorylation around 24 and 48 h after HI.

pSTAT3 Expression in the CC

At 3 and 12 h (fig. 3A–D) following hypoxia, some pSTAT3+ nuclei were located in the injured CC. At 24 h after hypoxia, its number increased mainly in the cingulum of the IL side and in the interconnection region of the CC with the CL hemisphere (fig. 3E, F). At 48 h after hypoxia, a higher expression of pSTAT3+ cells was observed, where they increased in all the IL CC and in the interconnection region of the hemispheres (fig. 3G, H). A decrease in pSTAT3+ cells was later observed at 72 h after hypoxia in all the CC (fig. 3I, J), and it continued to decline till 7 days after hypoxia, with very few pSTAT3+ cells in the injured CC (fig. 3K, L).

pSTAT3 Expression in the Hippocampus

pSTAT3+ cells were detected at 3 and 12 h after hypoxia in the injured IL hippocampal fissure and also in the fimbria (fig. 3B, D). At 24 h after hypoxia, an increase in pSTAT3+ cells was detected in the whole IL hippocampus, mainly in the hippocampal fissure (fig. 3F). At 48 h after hypoxia, the number of pSTAT3+ cells increased further, but they were located mainly in the cornu ammonis and dentate gyrus region with a few still in the hippocampal fissure and the fimbria (fig. 3H). The pSTAT3+ cells in the whole IL brain decreased from 72 h after HI, and only a few positive cells were detected in the hippocampus (fig. 3J). At 7 days after HI, there were still some pSTAT3+ cells in the atrophied IL hippocampus (fig. 3L). The CL side showed no significant pSTAT3 expression.

pSTAT3 Expression in the Caudate-Putamen, Neocortex and Thalamus

No pSTAT3+ cells were detected in the neocortex or in the thalamus, neither in the IL nor in the CL hemispheres. Only a few pSTAT3+ cells were detected in the IL caudate-putamen from 3 to 72 h after hypoxia. As in the CC or the hippocampus, the maximal expression was observed at 48 h after HI in the IL hemisphere (data not shown).

pSTAT3 Was Expressed by a Subpopulation of Astrocytes and Microglia/Macrophages in the IL Hemisphere

At all survival times analyzed after HI, a phosphorylated and activated form of STAT3 in the nuclei was detected, mainly in the CC (fig. 4D–H, 5D–H) and in the hippocampus of the IL hemisphere (fig. 5). pSTAT3+ nuclei co-localized with GFAP as early as 3 h after hypoxia (data not shown) and were identified as astrocytes (fig. 4D–H, 5D–H; see insets). There were some F4/80+ microglia/macrophages co-localizing with pSTAT3 appearing from 12 h onwards (fig. 4D–H, 5D–H; see insets). The morphology of pSTAT3+ cells was activated ramified and ameboid microglia in the gray matter, while the pSTAT3+ microglia in the white matter were predominantly ameboid. It should be noted that pSTAT3+ astrocytes or microglia/macrophages were always a subpopulation of the reactive cells analyzed.

Quantification of Active pSTAT3

After the immunohistochemistry, we quantified the pSTAT3 progression following HI by Western blot analysis. Antibody to pSTAT3 detected a single protein band (85 kDa) in nuclear extracts derived from control and injured brain samples (fig. 6). Densitometric analysis of pSTAT3 bands revealed increases immediately after HI, maximizing around 12–24 h and gradually decreasing thereafter (fig. 6; vs. respective controls). Statistical significance was achieved from 3 to 72 h, between the IL and CL hemisphere (fig. 6; IL vs. CL) after HI and also with respect to the age-matched controls (fig. 6; vs. respective controls). The values became comparable to control from 72 h onwards.

Discussion

The cytokine location in the brain is known to play a vital role in the outcome of any immune response. We have previously described colossal damage and cellular changes in both hemispheres following HI to neonatal mouse brain in the short and long term [19]. Following the conduct, the present study evaluates the expression of cytokines and the activation of transcription factor STAT3 (measuring pSTAT3) in the same HI model. pSTAT3 activation was observed in a subpopulation of astrocytes and activated microglia. Interestingly, pSTAT3

Fig. 4. Spatiotemporal expression pattern of pSTAT3 in astrocytes and microglia of white matter as revealed by immunofluorescence. Representative drawing of the white matter region analyzed (**A**). pSTAT3 (red), astrocyte marker GFAP (blue), activated microglia marker F4/80 (green) and nuclear marker DAPI (blue), immunofluorescence in the P7 control (**B**) and P14 control white matter (**C**), 12 h (**D**), 24 h (**E**), 48 h (**F**), 72 h (**G**) and 7 days (**H**) after hypoxia. The insets under the time points show a magnified image of a pSTAT3+ astrocyte in the upper lane (') and a pSTAT3+ microglia/macrophage in the lower lane ('). Scale bar: 5 μm.

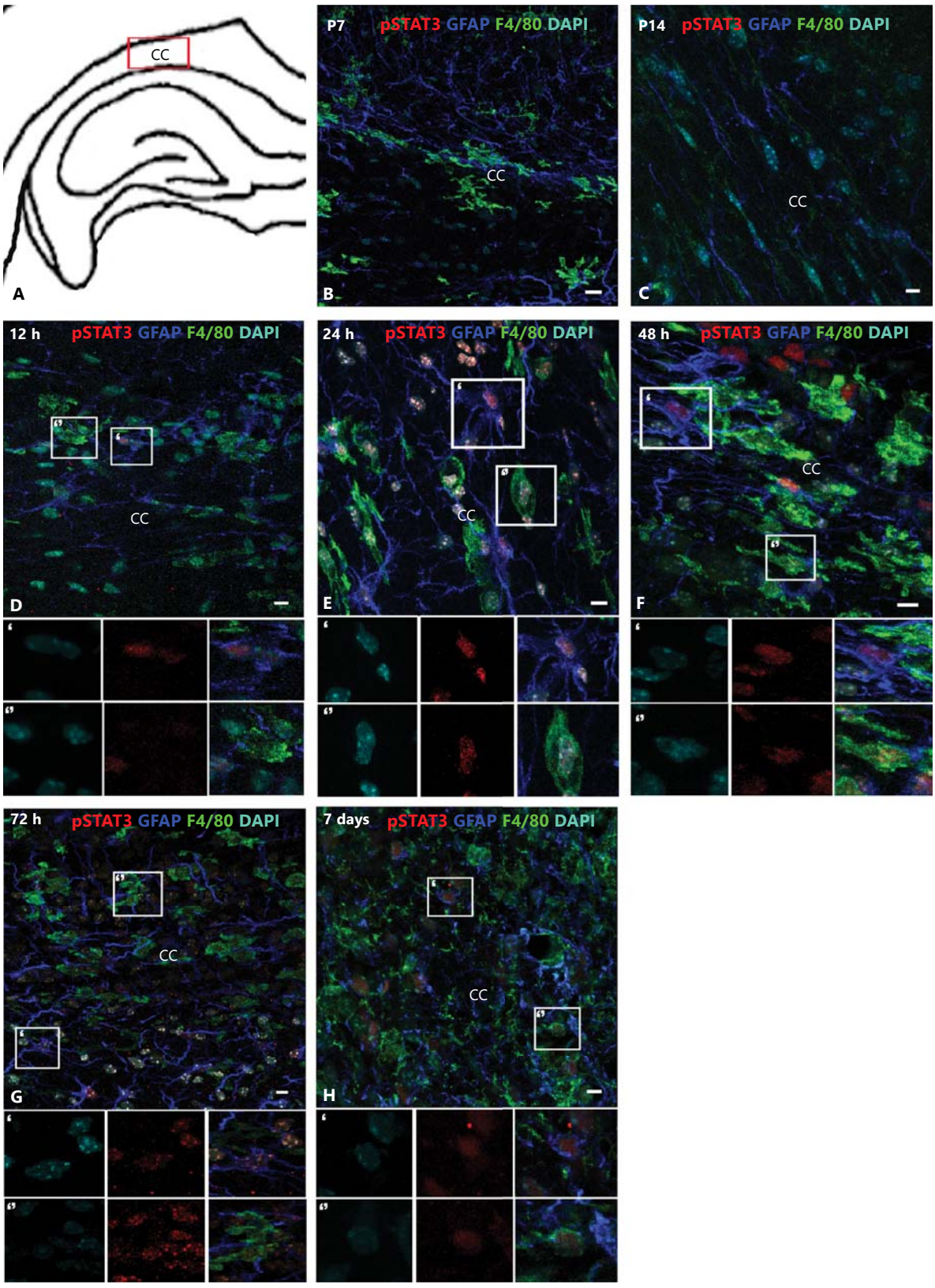
CC
A
P7 pSTAT3 GFAP F4/80 DAPI
CC
B
P14 pSTAT3 GFAP F4/80 DAPI
CC
C
12 h pSTAT3 GFAP F4/80 DAPI
CC
D
24 h pSTAT3 GFAP F4/80 DAPI
CC
E
48 h pSTAT3 GFAP F4/80 DAPI
CC
F
72 h pSTAT3 GFAP F4/80 DAPI
CC
G
7 days pSTAT3 GFAP F4/80 DAPI
CC
H

4

is only observed in the IL hemisphere especially in the hippocampus and CC. Meanwhile, changes in IL-6, the inducer of activation of STAT3, and the effectors of inflammatory response such as IL-1ra, IL-4 and IL-13 were observed in the IL as well as the CL hemisphere.

It is well known that HI leads to inflammation-induced secondary damage. Therefore, we made an effort to follow the pro- and anti-inflammatory cytokine response correlating with the damage. IL-6 and IL-10 are important regulators of cytokine production by astrocytes in the brain, and can control the production of TNF-α [37]. We observed the presence of IL-6 in the postnatal brain at low levels in line with previous reports [38]. We also noticed a sharp increase in IL-6 following HI as early as 3–12 h after hypoxia in the IL hemisphere, as also previously reported in adult rats following cerebral ischemia [39] though there is a scarcity of data in neonates. Microglial activation has been reported at early times in our previous reports [19], which is speculated to be releasing IL-6. As the level of IL-10 was not significant at any stage in our study, IL-6 may be the major cytokine attributed to provide a check on the TNF-α level in the injured brain.

In agreement with previous reports by Hedtjarn et al. [40], we saw IL-1β differentially rising quite early in the IL hemisphere, which is otherwise undetectable in the neonatal or adult brain [41]. In humans, elevated levels of IL-1β were associated with the severity of HI encephalopathy [42]. The expression of IL-1β in microglia has been reviewed by McAdams and Juul [43] hence showing a correlation between the temporal expressions of activated microglia and IL-1β in our model. A persistent increase in IL-1β as seen in both hemispheres is supposed to be the result of hypoxia per se, as no cumulative effect was observed at later time points. Studies suggest that microglial expression of IL-1β may lead to the vicious cycle of astrogliosis [44] as we had shown an increased number of activated microglia/macrophages and infiltrating neutrophils at later time points [19].

IL-4, IL-10, IL-1ra and IL-13 are potent anti-inflammatory agents with the ability to suppress the expression of IL-1β and TNF-α [45]. Our analysis depicted a considerable alteration in their expression following HI. Previous reports suggest that IL-13 and IL-4 induce death of activated microglia preventing chronic inflammation [46, 47]. We found a significant increase in IL-4 and IL-13 with no significant differences between the hemispheres, probably highlighting the global endogenous defense to counteract the inflammatory phenomenon initiated in the brain by hypoxia per se. Furthermore, IL-4 and IL-13 have been reported to share receptors [48], hence they might perform and express in a similar fashion as revealed by a long-term expression in our study. Still the changes on microglia viability in neonatal HI and its correlation with IL-13 expression need to be elucidated.

An important role of IL-4, as reviewed by Colton [49], is the switch of macrophage to an anti-inflammatory phenotype (M2 subset). Also, middle cerebral artery occlusion-induced Th1 polarization in IL-4 knockout mice had been associated with injury [50]. We assume a trend towards such a switch in macrophages/microglia during the later stages of HI, which was in accordance with the increase in IL-1ra at these time points. Interestingly, significantly high levels of IL-1ra in the IL hemisphere signal towards a combined effect of a micro- and astrogliosis-induced inflammatory milieu that needs to be counteracted. A previously observed reduction in activated microglia and astrocytes 7 days after hypoxia [19] and suppressed levels of TNF-α in the current study may be attributed to an increase in IL-4 and IL-13 leading to reduced inflammation. Further study to decipher their mechanism is needed.

Astrocytes respond to HI quite early and have been associated with the pathophysiological events leading to brain damage [51, 52]. Hence we quantified the changes in GFAP expression, if any, following HI to have an estimate of ongoing astrogliosis. Our results depict that there was an increase in GFAP persisting till 7 days after hypoxia in the IL hemisphere, in accordance with our previous reports [19]. Further exploring the signaling pathway involved, we analyzed the spatiotemporal expression of pSTAT3. Although STAT3 is expressed throughout the rat brain during development [53, 54], we did not observe pSTAT3 activation in mice, which can be attributed to species/strain-related variations. We observed activation of pSTAT3 in the CC and the hippocampal fissure from where the expression seemed to spread in all the IL hippocampus as injury progressed. This follows the pattern of initiation and expansion of astro- and microgliosis in the IL side, along with the neutrophil infiltration described

Fig. 5. Co-localization of pSTAT3 with astrocytes and microglia markers in gray matter as seen by immunofluorescence. Representative drawing of the gray matter region analyzed (**A**). pSTAT3 (red), astrocyte marker GFAP (blue), activated microglia marker F4/80 (green) and nuclear marker DAPI (blue), immunofluorescence in the P7 control (**B**) and P14 control gray matter (**C**), 12 h (**D**), 24 h (**E**), 48 h (**F**), 72 h (**G**) and 7 days (**H**) after HI. Insets under the time points are magnified details of a pSTAT3+ astrocyte in the upper lane (') and a pSTAT3+ microglia/macrophage in the lower lane (''). CA = Cornu ammonis; hif = hippocampal fissure. Scale bar: 5 μm.

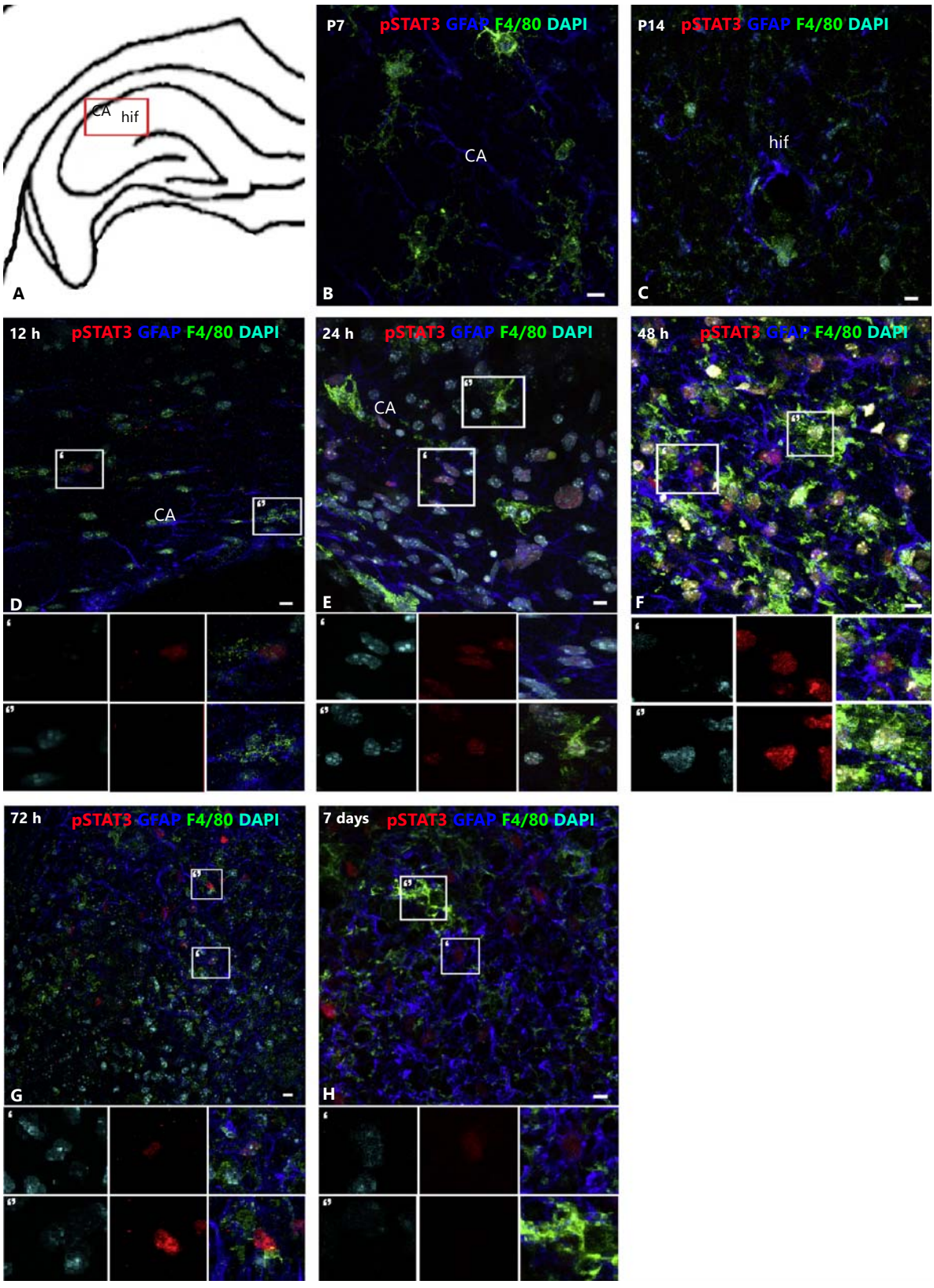

Color version available online

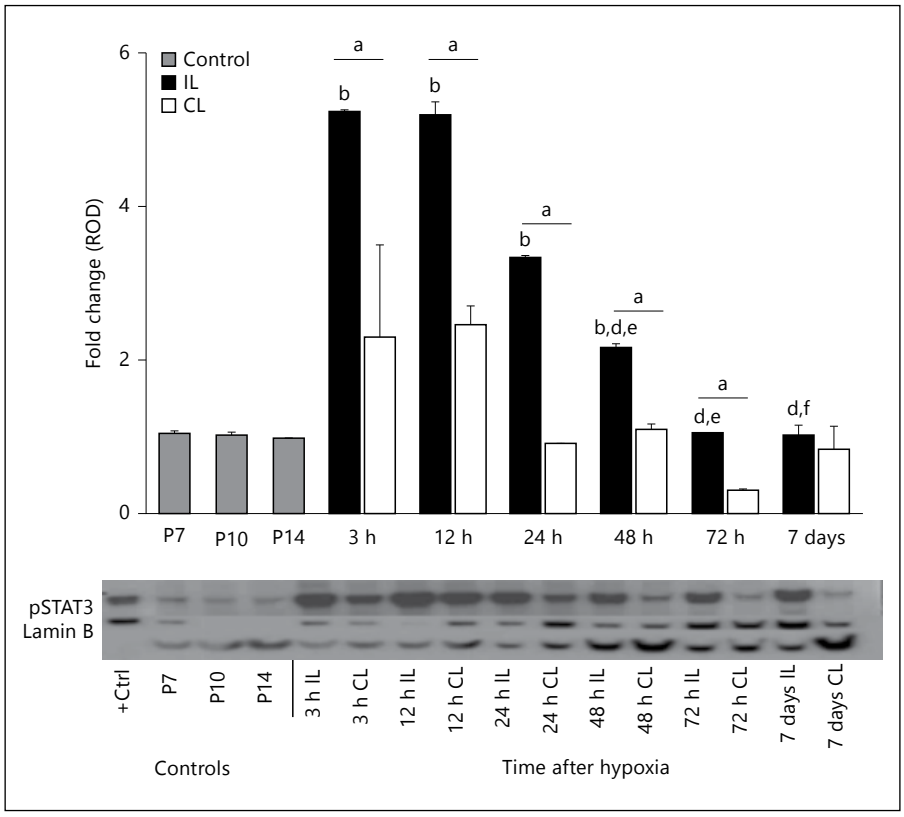

Fig. 6. Densitometric analyses of pSTAT3 Western blot in developing mouse brain following HI with respect to age-matched controls (P7, P10 and P14). Representative Western blot of pSTAT3 and Lamin B, the latter used for normalization of protein loading shown in the graph as relative optical density (ROD). The concentration of pSTAT3 increased after HI significantly in the IL as compared to the CL hemisphere, which later became comparable to controls by 7 days after hypoxia. Data are means ± SEM. Significant differences between groups were determined by analysis of variance followed by Bonferroni post hoc test or t test. [a] $p < 0.05$, IL versus CL); [b] $p < 0.05$, versus P7; [d] $p < 0.05$, versus 3 h IL; [e] $p < 0.01$, versus 12 h IL, and [f] $p < 0.05$, versus 24 h IL after HI.

in our previous study [19]. STAT3 has been shown to play a crucial role in the neutrophil mobilization response in the periphery [55], but such a role in the central nervous system is yet to be explored.

To the best of our knowledge, this is the first study that describes the pSTAT3 activation after neonatal HI in mice. In our HI model, we perceive the maximum nuclear expression of pSTAT3 around 24–48 h after hypoxia, as seen by immunofluorescence staining in the IL side in accordance with a previous study in adult mice after lesion [56, 57]. Our Western blot data point towards a much earlier peak of pSTAT3 expression in the IL hemisphere (3–12 h after hypoxia). This difference could be attributed to the fact that the whole IL/CL hemisphere was used to prepare the nuclear extract due to the smaller size of the neonatal brain tissue, which might have diluted the effect in the atrophied region. We identified the cells showing pSTAT3+ nuclei as a subpopulation of astrocytes and microglia/macrophages in the IL hemisphere. Although there is a scarcity of data regarding cellular expression in a neonatal HI model in mice, there are reports suggesting increased expression of STAT3 in astroglial cells after adult brain damage [58].

Cattaneo et al. [22] have shown robust STAT3 activity preceding the onset of astrogliogenesis. We observed pSTAT3 activation preceding, at least in part, the increase in GFAP, which has also been described in ischemic adult brain [59]. Studies show a mechanism where the Jak/Stat pathway involving pSTAT3 was crucial in the activation of GFAP in astrocytes [60, 61]. STAT3 activation in astrocytes had indirectly been linked to neuronal survival after ischemia [62–64]. A neuroprotective or damaging role of astrogliosis is yet to be elaborated in the model under study.

Notably, we observed pSTAT3 expressing microglia/macrophages, which are considered as a main source of inflammatory cytokines, in the IL hemisphere. pSTAT3 activation in glia remains high till 7 days after hypoxia (only observed in confocal micrographs) pointing towards the role of STAT3 in the delayed inflammatory response, as also shown by Yi et al. [65]. Previous reports suggest that the mechanism of neuroprotection by endogenous IL-6 may be mediated via STAT3 [66]. In this study, the level of IL-6 could be correlated with an increase in pSTAT3+ astrocytes, as well as an extended astrogliosis in our model. Also, we hypothesized that this

increase in IL-6 in the milieu leads to a later pSTAT3 activation in microglia/macrophages; however, the role of IL-6 in our model needs to be expanded.

In summary, our study highlights a concurrent micro- and astrogliosis stating that the multifactorial and interdependent effect of the inflammatory response leads to HI-related pathology. A spatiotemporal activation of pSTAT3 following neonatal HI in mice brain during short and long term is described. A pattern of cytokines directly or indirectly regulated by STAT3 is also studied in a time-dependent manner. The potential pro-inflammatory cytokines showing immediate changes were IL-6 and IL-1β and the anti-inflammatory cytokines showing a long-term increase were IL-1ra, IL-4 and IL-13. We also support the notion of IL-6 and IL-1β being important biomarkers in HI-induced injury in the immature brain. Although further elucidation is still necessary, the fact that signaling pathways in glial cells utilized by above-mentioned cytokines might converge on STAT3 strongly advocates its role in the evolution of damage after hypoxia in the model studied. We suggest that while choosing inflammatory molecules as therapeutic targets, the time of intervention is the key factor and a global approach to balance the pro- and anti-inflammatory cytokines must be taken.

Acknowledgements

This study was supported by BFU2009-08805 from the Ministry of Science and Innovation, Government of Spain and Fundación La Marató de TV3 2011-110531. K. Shrivastava holds a postdoctoral fellowship from Fundación La Marató de TV3 and Universitat Autonoma Barcelona. M. Chertoff holds a Marie Curie International Incoming fellowship (2009-IIF-253110). We greatly appreciate the technical help from Miguel A. Martil, Isabella Appiah and Aushon BioSystems (Billerica, Mass., USA). We also thank Ms. Anna and Dr. J. Muntaner from 'The Vall d'Hebron University Hospital', Barcelona, for their help during standardization of protein array. Confocal analysis was carried out in the 'Servei Microscopia' of UAB.

References

1 Holling EE, Leviton A: Characteristics of cranial ultrasound white-matter echolucencies that predict disability: a review. Dev Med Child Neurol 1999;41:136–139.
2 Platt MJ, Cans C, Johnson A, Surman G, Topp M, Torrioli MG, Krageloh-Mann I: Trends in cerebral palsy among infants of very low birthweight (<1,500 g) or born prematurely (<32 weeks) in 16 European centres: a database study. Lancet 2007;369:43–50.
3 Robertson CM, Finer NN, Grace MG: School performance of survivors of neonatal encephalopathy associated with birth asphyxia at term. J Pediatr 1989;114:753–760.
4 Robertson CM, Grace MG: Validation of prediction of kindergarten-age school-readiness scores of nondisabled survivors of moderate neonatal encephalopathy in term infants. Can J Public Health 1992;83(suppl 2):S51–S57.
5 Woodward LJ, Edgin JO, Thompson D, Inder TE: Object working memory deficits predicted by early brain injury and development in the preterm infant. Brain 2005;128:2578–2587.
6 Allin M, Walshe M, Fern A, Nosarti C, Cuddy M, Rifkin L, Murray R, Rushe T, Wyatt J: Cognitive maturation in preterm and term born adolescents. J Neurol Neurosurg Psychiatry 2008;79:381–386.
7 Ferriero DM: Neonatal brain injury. N Engl J Med 2004;351:1985–1995.
8 Vannucci SJ, Hagberg H: Hypoxia-ischemia in the immature brain. J Exp Biol 2004;207:3149–3154.
9 Shankaran S, Pappas A, McDonald SA, Vohr BR, Hintz SR, Yolton K, Gustafson KE, Leach TM, Green C, Bara R, Petrie Huitema CM, Ehrenkranz RA, Tyson JE, Das A, Hammond J, Peralta-Carcelen M, Evans PW, Heyne RJ, Wilson-Costello DE, Vaucher YE, Bauer CR, Dusick AM, Adams-Chapman I, Goldstein RF, Guillet R, Papile LA, Higgins RD: Childhood outcomes after hypothermia for neonatal encephalopathy. N Engl J Med 2012;366:2085–2092.
10 Gonzalez FF, Ferriero DM: Therapeutics for neonatal brain injury. Pharmacol Ther 2008;120:43–53.
11 Jenkins DD, Rollins LG, Perkel JK, Wagner CL, Katikaneni LP, Bass WT, Kaufman DA, Horgan MJ, Languani S, Givelichian L, Sankaran K, Yager JY, Martin RH: Serum cytokines in a clinical trial of hypothermia for neonatal hypoxic-ischemic encephalopathy. J Cereb Blood Flow Metab 2012;32:1888–1896.
12 Alvarez-Diaz A, Hilario E, de Cerio FG, Valls-i-Soler A, Alvarez-Diaz FJ: Hypoxic-ischemic injury in the immature brain – Key vascular and cellular players. Neonatology 2007;92:227–235.
13 Dammann O, Durum S, Leviton A: Do white cells matter in white matter damage? Trends Neurosci 2001;24:320–324.
14 Northington FJ, Chavez-Valdez R, Martin LJ: Neuronal cell death in neonatal hypoxia-ischemia. Ann Neurol 2011;69:743–758.
15 Vexler ZS, Yenari MA: Does inflammation after stroke affect the developing brain differently than adult brain? Dev Neurosci 2009;31:378–393.
16 Faustino JV, Wang X, Johnson CE, Klibanov A, Derugin N, Wendland MF, Vexler ZS: Microglial cells contribute to endogenous brain defenses after acute neonatal focal stroke. J Neurosci 2011;31:12992–13001.
17 Cuadros MA, Navascues J: The origin and differentiation of microglial cells during development. Prog Neurobiol 1998;56:173–189.
18 Vaccarino FM, Fagel DM, Ganat Y, Maragnoli ME, Ment LR, Ohkubo Y, Schwartz ML, Silbereis J, Smith KM: Astroglial cells in development, regeneration, and repair. Neuroscientist 2007;13:173–185.
19 Shrivastava K, Chertoff M, Llovera G, Recasens M, Acarin L: Short and long-term analysis and comparison of neurodegeneration and inflammatory cell response in the ipsilateral and contralateral hemisphere of the neonatal mouse brain after hypoxia/ischemia. Neurol Res Int 2012;2012:781512.
20 Planas AM, Gorina R, Chamorro A: Signalling pathways mediating inflammatory responses in brain ischaemia. Biochem Soc Trans 2006;34:1267–1270.
21 Nicolas CS, Peineau S, Amici M, Csaba Z, Fafouri A, Javalet C, Collett VJ, Hildebrandt L, Seaton G, Choi SL, Sim SE, Bradley C, Lee K, Zhuo M, Kaang BK, Gressens P, Dournaud P, Fitzjohn SM, Bortolotto ZA, Cho K, Collingridge GL: The Jak/STAT pathway is involved in synaptic plasticity. Neuron 2012;73:374–390.

22 Cattaneo E, Conti L, De-Fraja C: Signalling through the JAK-STAT pathway in the developing brain. Trends Neurosci 1999;22:365–369.
23 De-Fraja C, Conti L, Magrassi L, Govoni S, Cattaneo E: Members of the JAK/STAT proteins are expressed and regulated during development in the mammalian forebrain. J Neurosci Res 1998;54:320–330.
24 Lucchese G, Cambi GE, De Rita F, Faggian G, Mazzucco A, Modesti PA, Luciani GB: Cardioplegia and angiotensin II receptor antagonists modulate signal transducers and activators of transcription activation in neonatal rat myocytes. Artif Organs 2011;35:1075–1081.
25 Fukushi S, Yamasaki K, Aiba S: Nuclear localization of activated STAT6 and STAT3 in epidermis of prurigo nodularis. Br J Dermatol 2011;165:990–996.
26 Elango C, Devaraj SN: Immunomodulatory effect of hawthorn extract in an experimental stroke model. J Neuroinflammation 2010;7:97.
27 Acarin L, González B, Castellano B: STAT3 and NFkappaB activation precedes glial reactivity in the excitotoxically injured young cortex but not in the corresponding distal thalamic nuclei. J Neuropathol Exp Neurol 2000;59:151–163.
28 Dziennis S, Alkayed NJ: Role of signal transducer and activator of transcription 3 in neuronal survival and regeneration. Rev Neurosci 2008;19:341–361.
29 Zhang X, Shan P, Alam J, Fu XY, Lee PJ: Carbon monoxide differentially modulates STAT1 and STAT3 and inhibits apoptosis via a phosphatidylinositol 3-kinase/Akt and p38 kinase-dependent STAT3 pathway during anoxia-reoxygenation injury. J Biol Chem 2005;280:8714–8721.
30 Rice JE 3rd, Vannucci RC, Brierley JB: The influence of immaturity on hypoxic-ischemic brain damage in the rat. Ann Neurol 1981;9:131–141.
31 Vannucci RC, Vannucci SJ: A model of perinatal hypoxic-ischemic brain damage. Ann NY Acad Sci 1997;835:234–249.
32 Hagberg H, Peebles D, Mallard C: Models of white matter injury: comparison of infectious, hypoxic-ischemic, and excitotoxic insults. Ment Retard Dev Disabil Res Rev 2002;8:30–38.
33 Sheldon RA, Sedik C, Ferriero DM: Strain-related brain injury in neonatal mice subjected to hypoxia-ischemia. Brain Res 1998;810:114–122.
34 Northington FJ: Brief update on animal models of hypoxic-ischemic encephalopathy and neonatal stroke. ILAR J 2006;47:32–38.
35 Vannucci RC, Connor JR, Mauger DT, Palmer C, Smith MB, Towfighi J, Vannucci SJ: Rat model of perinatal hypoxic-ischemic brain damage. J Neurosci Res 1999;55:158–163.
36 Kolbus A, Pilat S, Husak Z, Deiner EM, Stengl G, Beug H, Baccarini M: Raf1 antagonizes erythroid differentiation by restraining caspase activation. J Exp Med 2002;196:1347–1353.
37 Benveniste EN, Tang LP, Law RM: Differential regulation of astrocyte TNF-alpha expression by the cytokines TGF-beta, IL-6 and IL-10. Int J Dev Neurosci 1995;13:341–349.
38 Van Wagoner NJ, Benveniste EN: Interleukin-6 expression and regulation in astrocytes. J Neuroimmunol 1999;100:124–139.
39 Suzuki S, Tanaka K, Nogawa S, Nagata E, Ito D, Dembo T, Fukuuchi Y: Temporal profile and cellular localization of interleukin-6 protein after focal cerebral ischemia in rats. J Cereb Blood Flow Metab 1999;19:1256–1262.
40 Hedtjarn M, Leverin AL, Eriksson K, Blomgren K, Mallard C, Hagberg H: Interleukin-18 involvement in hypoxic-ischemic brain injury. J Neurosci 2002;22:5910–5919.
41 Rothwell NJ, Luheshi GN: Interleukin 1 in the brain: biology, pathology and therapeutic target. Trends Neurosci 2000;23:618–625.
42 Aly H, Khashaba MT, El-Ayouty M, El-Sayed O, Hasanein BM: IL-1beta, IL-6 and TNF-alpha and outcomes of neonatal hypoxic ischemic encephalopathy. Brain Dev 2006;28:178–182.
43 McAdams RM, Juul SE: The role of cytokines and inflammatory cells in perinatal brain injury. Neurol Res Int 2012;2012:561494.
44 Lee SC, Liu W, Dickson DW, Brosnan CF, Berman JW: Cytokine production by human fetal microglia and astrocytes. Differential induction by lipopolysaccharide and IL-1beta. J Immunol 1993;150:2659–2667.
45 Dinarello CA: Proinflammatory cytokines. Chest 2000;118:503–508.
46 Shin WH, Lee DY, Park KW, Kim SU, Yang MS, Joe EH, Jin BK: Microglia expressing interleukin-13 undergo cell death and contribute to neuronal survival in vivo. Glia 2004;46:142–152.
47 Yang MS, Park EJ, Sohn S, Kwon HJ, Shin WH, Pyo HK, Jin B, Choi KS, Jou I, Joe EH: Interleukin-13 and -4 induce death of activated microglia. Glia 2002;38:273–280.
48 Zurawski SM, Vega F Jr, Huyghe B, Zurawski G: Receptors for interleukin-13 and interleukin-4 are complex and share a novel component that functions in signal transduction. EMBO J 1993;12:2663–2670.
49 Colton CA: Heterogeneity of microglial activation in the innate immune response in the brain. J Neuroimmune Pharmacol 2009;4:399–418.
50 Xiong X, Barreto GE, Xu L, Ouyang YB, Xie X, Giffard RG: Increased brain injury and worsened neurological outcome in interleukin-4 knockout mice after transient focal cerebral ischemia. Stroke 2011;42:2026–2032.
51 Sen E, Levison SW: Astrocytes and developmental white matter disorders. Ment Retard Dev Disabil Res Rev 2006;12:97–104.
52 Sullivan SM, Bjorkman ST, Miller SM, Colditz PB, Pow DV: Morphological changes in white matter astrocytes in response to hypoxia/ischemia in the neonatal pig. Brain Res 2010;1319:164–174.
53 Gautron L, De Smedt-Peyrusse V, Laye S: Characterization of STAT3-expressing cells in the postnatal rat brain. Brain Res 2006;1098:26–32.
54 Murata S, Usuda N, Okano A, Kobayashi S, Suzuki T: Occurrence of a transcription factor, signal transducer and activators of transcription 3 (STAT3), in the postsynaptic density of the rat brain. Mol Brain Res 2000;78:80–90.
55 Nguyen-Jackson H, Panopoulos AD, Zhang H, Li HS, Watowich SS: STAT3 controls the neutrophil migratory response to CXCR2 ligands by direct activation of G-CSF-induced CXCR2 expression and via modulation of CXCR2 signal transduction. Blood 2010;115:3354–3363.
56 Suzuki S, Tanaka K, Nogawa S, Dembo T, Kosakai A, Fukuuchi Y: Phosphorylation of signal transducer and activator of transcription-3 (STAT3) after focal cerebral ischemia in rats. Exp Neurol 2001;170:63–71.
57 Satriotomo I, Bowen KK, Vemuganti R: JAK2 and STAT3 activation contributes to neuronal damage following transient focal cerebral ischemia. J Neurochem 2006;98:1353–1368.
58 Justicia C, Gabriel C, Planas AM: Activation of the JAK/STAT pathway following transient focal cerebral ischemia: signaling through JAK1 and STAT3 in astrocytes. Glia 2000;30:253–270.
59 Choi JS, Kim SY, Cha JH, Choi YS, Sung KW, Oh ST, Kim ON, Chung JW, Chun MH, Lee SB, Lee MY: Upregulation of gp130 and STAT3 activation in the rat hippocampus following transient forebrain ischemia. Glia 2003;41:237–246.
60 Bain JM, Ziegler A, Yang Z, Levison SW, Sen E: TGFbeta1 stimulates the over-production of white matter astrocytes from precursors of the 'brain marrow' in a rodent model of neonatal encephalopathy. PLoS One 2010;5:e9567.
61 Fukuda S, Abematsu M, Mori H, Yanagisawa M, Kagawa T, Nakashima K, Yoshimura A, Taga T: Potentiation of astrogliogenesis by STAT3-mediated activation of bone morphogenetic protein-Smad signaling in neural stem cells. Mol Cell Biol 2007;27:4931–4937.
62 Bambrick L, Kristian T, Fiskum G: Astrocyte mitochondrial mechanisms of ischemic brain injury and neuroprotection. Neurochem Res 2004;29:601–608.
63 Haber M, Zhou L, Murai KK: Cooperative astrocyte and dendritic spine dynamics at hippocampal excitatory synapses. J Neurosci 2006;26:8881–8891.
64 Nedergaard M, Dirnagl U: Role of glial cells in cerebral ischemia. Glia 2005;50:281–286.
65 Yi JH, Park SW, Kapadia R, Vemuganti R: Role of transcription factors in mediating post-ischemic cerebral inflammation and brain damage. Neurochem Int 2007;50:1014–1027.
66 Yamashita T, Sawamoto K, Suzuki S, Suzuki N, Adachi K, Kawase T, Mihara M, Ohsugi Y, Abe K, Okano H: Blockade of interleukin-6 signaling aggravates ischemic cerebral damage in mice: possible involvement of STAT3 activation in the protection of neurons. J Neurochem 2005;94:459–468.